Polymer 51 (2010) 3431–3435

Contents lists available at ScienceDirect

Polymer

journal homepage: www.elsevier.com/locate/polymer

Synthesis and characterization of layer-aligned poly(vinyl alcohol)/graphene nanocomposites

Xiaoming Yang [a,c], Liang Li [b,c,**], Songmin Shang [c,*], Xiao-ming Tao [c]

[a] College of Chemistry, Chemical Engineering and Materials Sciences, Soochow University, Suzhou 215123, China
[b] Key Laboratory for Green Chemical Process of Ministry of Education, School of Materials Science and Engineering, Wuhan Institute of Technology, Wuhan 430073, China
[c] Institute of Textiles and Clothing, The Hong Kong Polytechnic University, Hong Kong, China

ARTICLE INFO

Article history:
Received 26 February 2010
Received in revised form
21 April 2010
Accepted 19 May 2010
Available online 26 May 2010

Keywords:
Nanocomposites
Thermal properties
Mechanical properties

ABSTRACT

Layer-aligned poly(vinyl alcohol)/graphene nanocomposites in the form of films are prepared by reducing graphite oxide in the polymer matrix in a simple solution processing. X-ray diffractions, scanning electron microscopy, Fourier-transform infrared spectroscopy, differential scanning calorimetry and thermogravimetric analysis are used to study the structure and properties of these nanocomposites. The results indicate that graphene is dispersed on a molecular scale and aligned in the poly(vinyl alcohol) (PVA) matrix and there exists strong interfacial interactions between both components mainly by hydrogen bonding, which are responsible for the change of the structures and properties of the PVA/graphene nanocomposites such as the increase in T_g and the decrease in the level of crystallization.

1. Introduction

Graphene, as a single layer of carbon atoms in a two-dimensional honeycomb crystal lattice, has been attracting tremendous interest in the fields of electronics and composite materials because of its fascinating properties [1,2]. It has been found that electrons move ballistically in the graphene structure with a mobility exceeding 15,000 $m^2V^{-1}s^{-1}$ [3]. Theoretical and experimental results show that single-layered graphene sheets are the strongest materials developed thus far [4]. Graphene nanosheets also have high thermal conductivity and high specific surface area [5]. These particular properties make graphene an excellent additive to dramatically enhance the mechanical, thermal, and electrical properties of polymer materials [6–8]. Great efforts have been made in the use of solution-processable graphene materials for highly conducting composite [9], transparent electrode [10], and photovoltaic device [11] applications.

So far, technological and engineering applications of graphene sheets usually require graphene solutions (or dispersions) either in water or in an organic solvent. However, as-prepared graphene itself is not soluble and therefore, cannot be dispersed in water or in any organic solvent. A main challenge for realizing the large-scale potential for polymer/graphene nanocomposites is to homogeneously disperse thin nanosheets of graphene within the polymeric matrix. Moreover, the control of the interfacial interaction is crucial. In this respect, graphene oxide (GO), the oxygenated counterpart of graphene, has already been explored as an attractive intermediate to synthesize graphene nanocomposites [12]. GO bears various oxygen functional groups (e.g. hydroxyl, epoxide, and carbonyl groups) covalently bonded on their basal planes and edges of carbon atoms. Therefore, GO is hydrophilic and can be readily dispersed in water as individual sheets to form stable colloidal suspensions [13]. Meanwhile, these oxygen-containing groups impart GO sheets with the function of strong interaction with polar small molecules or polymers to form GO intercalated or exfoliated composites [14,15]. More important, GO can be readily reduced chemically to graphene by a variety of common reagents [16–18].

Herein, we report an investigation into the aqueous solution processing of graphene nanosheets in the polymer matrix. A simple and practical approach to synthesize well-dispersed nanocomposites with aligned graphene nanosheets in a poly(vinyl alcohol) (PVA) matrix is demonstrated. The effect of graphene content on the structures and properties of PVA/graphene nanocomposites is investigated. Although the addition of graphene significantly decreases the crystallinity of PVA matrix, the film of the PVA/graphene nanocomposite is strong and ductile. These results demonstrate that the change of structure and properties of the PVA/graphene nanocomposites could be ascribed to the

* Corresponding author. Tel.: +852 6979 3168; fax: +852 2773 1432.
** Corresponding author.
E-mail addresses: msell08@163.com (L. Li), tcshang@inet.polyu.edu.hk (S. Shang).

0032-3861/$ – see front matter © 2010 Elsevier Ltd. All rights reserved.
doi:10.1016/j.polymer.2010.05.034

uniform dispersion on a molecular scale and alignment of graphene in the polymer matrix and strong interfacial interactions between both components.

2. Experiment

2.1. Materials

Graphite powder was purchased from Uni-Chem. PVA (99+% hydrolyzed, M_w ~ 89,000–98,000) and hydrazine (~35% water solution) were purchased from Aldrich. Other reagents were of analytical grade and used without further purification.

2.2. Synthesis of PVA/graphene nanocomposites

GO was synthesized from graphite powder by the modified Hummers method [19,20]. The procedures for preparing PVA/graphene nanocomposite films are described as follows. GO was dissolved in 10 mL of water and treated with ultrasound for 45 min to make a homogeneous brown dispersion (1 mg/mL). PVA powder was dissolved in distilled water at 90 °C and the solution was subsequently cooled to room temperature. The GO aqueous dispersion was gradually added to the PVA solution and sonicated at room temperature for 15 min and stirred to obtain homogeneous PVA/GO solutions. Then, the reduction of GO was accomplished by adding hydrazine to the PVA/GO solution and keeping it under magnetic stirring at 100 °C for 24 h. Finally, the above solutions were cast into glass dishes and kept at 40 °C for film formation until its weight equilibrated. The weight contents of graphene in the nanocomposite films described above were controlled to be 0.5, 1, 2 and 3.5 wt%. The above is designated as one-step approach.

For comparison, in two-step approach, only GO was first reduced by hydrazine to form graphene. Then, the as-prepared graphene were added and sonicated in PVA aqueous solution for 3 h, and then treated in an identical fashion similar to that described above in one-step approach.

2.3. Characterization

X-ray diffraction (XRD) was carried out using a PHILIPS PW 3710 diffractometer using Cu Kα radiation source ($\lambda = 1.54$ Å). Fourier-transform infrared spectra (FTIR) were obtained on a Perkin Elmer spectrum 100 FTIR spectrometer with a 4 cm^{-1} resolution. The glass transition and crystallization behaviors were investigated by differential scanning calorimetry (DSC) using a Perkin Elmer Pyris 1. The experiments were carried out in nitrogen atmosphere using about 5 mg sample sealed in aluminium pans. The samples were heated from room temperature to 240 °C, maintained at this temperature for 5 min, then cooled to room temperature and heated again to 240 °C. The heating and cooling rates were 10 °C/min in all cases. The glass transition temperatures and melting enthalpy are taken from the second heating run in the calorimetric curves. Thermogravimetric analysis (TGA) was performed on a Netzch STA 449C instrument at a heating rate of 10 °C/min in an air atmosphere. Scanning electron microscopy (SEM, JEOL Model JSM-6490) was used to observe the failure surfaces of the PVA/graphene nanocomposite films after tensile tests. The failure surfaces were coated with gold before analysis. The mechanical properties of PVA/graphene nanocomposite films were measured on a universal tensile testing machine (Instron 4411) at 20 °C with 60% relative humidity. The specimen dimension was 60 mm in

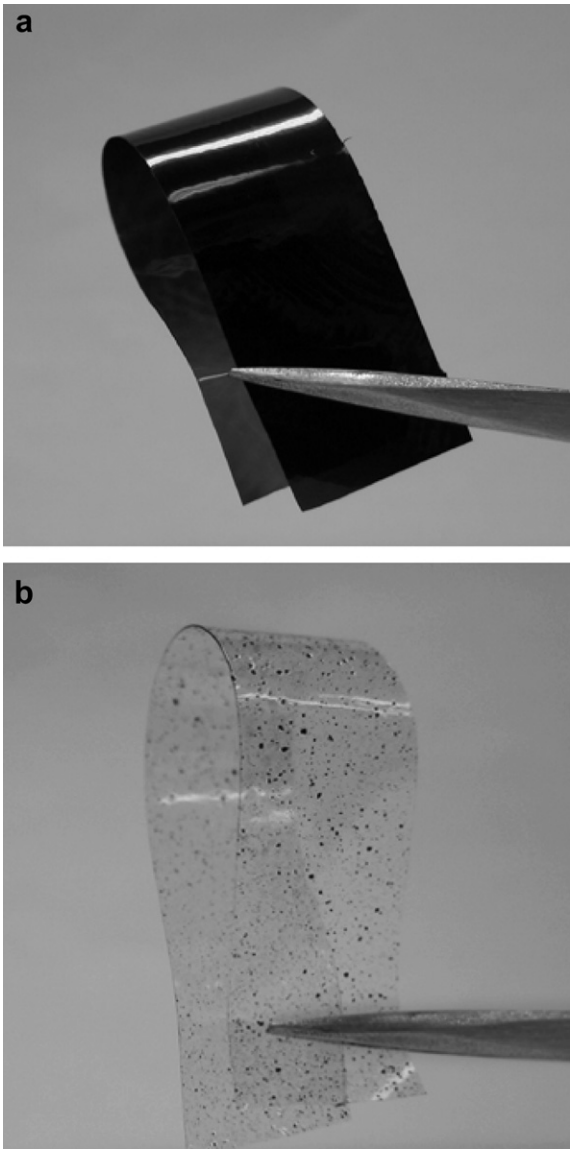

Fig. 1. Photographs of PVA/1 wt% graphene nanocomposite films prepared by (a) one-step and (b) two-step approach.

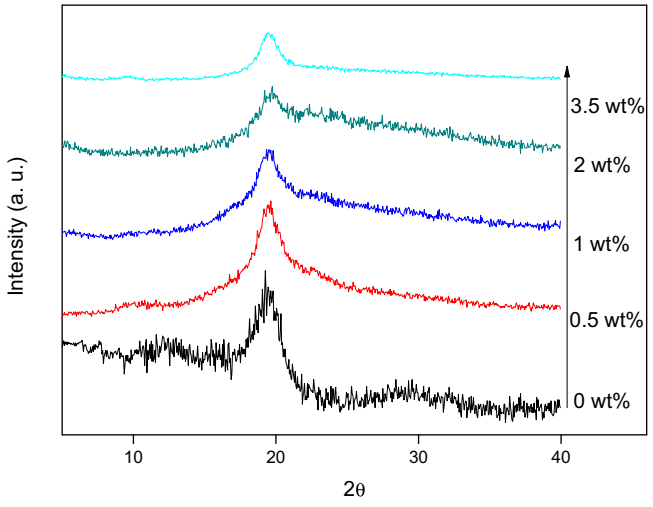

Fig. 2. XRD patterns of PVA/graphene nanocomposites with different graphene contents.

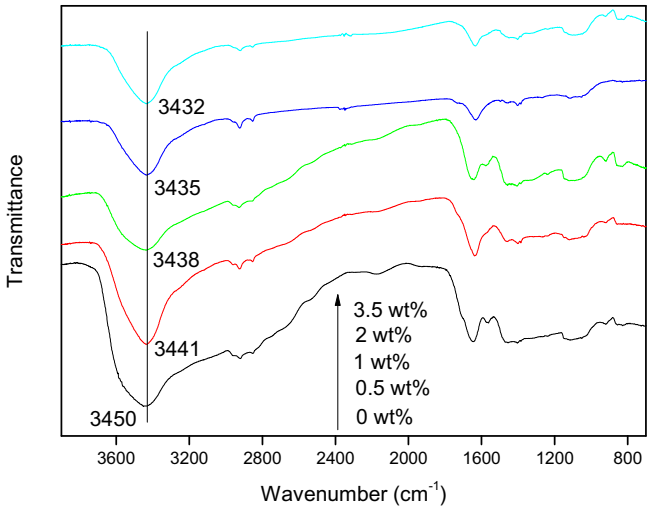

Fig. 3. FTIR spectra of PVA/graphene nanocomposites with different graphene contents.

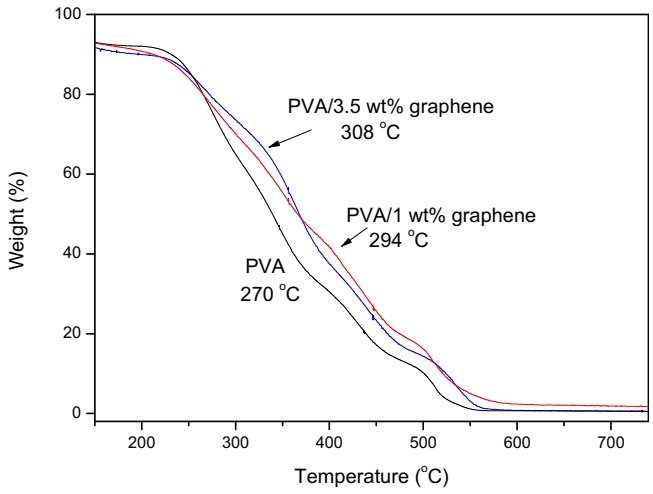

Fig. 4. TGA curves of PVA, PVA/1 wt% graphene nanocomposite and PVA/3.5 wt% graphene nanocomposite.

length, 10 mm in width, and 0.04 mm in thickness. The extension rate was 5 mm/min and the load cell was 250 N with a gauge length of 40 mm. The data on modulus, tensile stress and strain at rupture were the averages of five strips of the same sample. All the failure occurred at the middle region of the testing strips.

3. Results and discussion

In one-step approach, when hydrazine was added, the brownish solution of PVA/GO changed immediately to black, suggesting graphene formation by reduction of GO. Moreover, no precipitate was observed a few hours after the magnetic stirring had been stopped, which indicated that no aggregates of the graphene sheets were formed. This behavior suggests the presence of interactions between the PVA matrix and graphene for avoiding graphene sheets aggregation. Fig. 1 shows the photographs of PVA/1 wt% graphene nanocomposite films prepared by one-step and two-step approach, respectively. It can be seen that the film prepared by one-step approach is shining, smooth, uniform and flexible. However, there are obvious aggregations of black graphene in the film prepared by two-step approach. It suggests that it is difficult to disperse graphene uniformly in the polymer matrix in the case of two-step approach and the aggregation of graphene inevitably occurs. Therefore unless otherwise mentioned, the PVA/graphene nanocomposite films are prepared by one-step approach.

The structures of these films are studied by XRD. The characteristic XRD diffraction peak of pure GO sheets appears at $2\theta = 11.1^{\circ}$ with a d-spacing of 0.78 nm. After the formation of graphene by reducing GO in the presence of hydrazine, the XRD pattern of the graphene sheets shows the disappearance of the 11.1° peak confirming the complete reduction of the GO sheets (Fig. S1) [21]. XRD patterns of PVA/graphene nanocomposites with different graphene contents are shown in Fig. 2.

Table 1
Glass transition temperature and melting parameters of PVA and PVA/graphene nanocomposites.

Samples	T_g (°C)	ΔH_m(J/g)	X_c (%)[a]	ΔH_c(J/g)	T_m (°C)	T_c (°C)
PVA	76.2	53.1	38.3	56.3	230.2	200.0
PVA/0.5 wt% graphene	79.4	27.9	20.1	31.6	229.8	196.9
PVA/1 wt% graphene	84.3	25.1	18.1	29.4	229.6	195.7
PVA/2 wt% graphene	86.6	23.2	16.7	25.1	229.2	196.5
PVA/3.5 wt% graphene	90.5	7.8	5.6	11.2	228.9	198.4

[a] Obtained from the melting endotherms.

PVA shows diffraction peaks at 11.3, 19.4 and 22.4° that correspond to the crystalline phase of the polymer [22]. In the nanocomposites, the peaks at 11.3 and 22.4° disappear and the main peak at 19.4° decreased and became broader, showing a decrease in crystallinity and indicating that some interactions between polymer chains and the filler may take place.

FTIR experiments are performed to determine the interaction between polymer matrix and graphene sheets. It is well known that both the –OH stretching and the –C–OH stretching bands are sensitive to the hydrogen bonding. As shown in Fig. 3, the band around 3100–3500 cm^{-1}, involving the strong hydroxyl band for free and hydrogen bonded alcohols, shifts to a lower wavenumber with the increase of graphene contents in the PVA matrix. It could be ascribed to the dissociation of the hydrogen bonding among the hydroxyl groups in the polymer [23,24]. These results suggest that there exists hydrogen bonding between the polymer and graphene to the detriment of hydrogen bonding among polymer chains and diminishes the crystallinity of the polymer.

The glass transition and crystallization behavior of the polymer matrix in the nanocomposites are also investigated because the

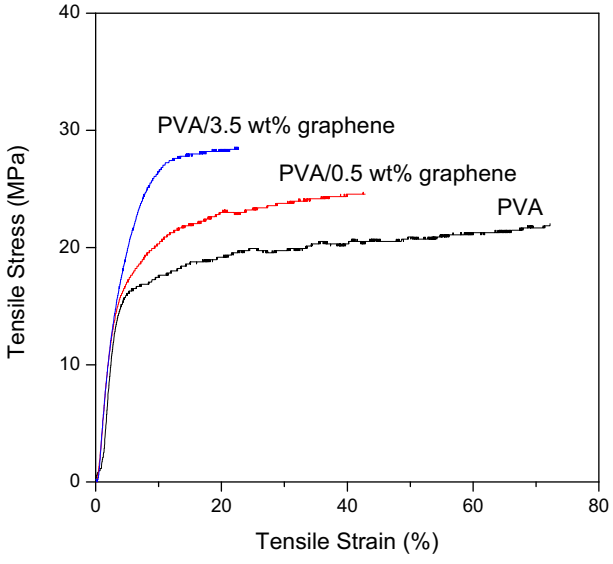

Fig. 5. Typical stress–strain behaviors for the films of PVA, PVA/0.5 wt% graphene nanocomposite and PVA/3.5 wt% graphene nanocomposite.

Table 2
Tensile properties of pure PVA and PVA/graphene nanocomposite films.

Samples	Tensile stress (MPa)	Modulus (GPa)	Tensile strain (%)
PVA	22 ± 1	0.45 ± 0.2	72 ± 6
PVA/0.5 wt% graphene	25 ± 2	0.48 ± 0.2	42 ± 5
PVA/3.5 wt% graphene	29 ± 2	0.52 ± 0.3	22 ± 2

macroscopic properties of the nanocomposites strongly depend on them. As shown in Table 1, significant changes can be observed in the glass transition temperature (T_g), the melting enthalpy (ΔH_m) and the cold crystallization enthalpy (ΔH_c) of PVA in the nanocomposites with different graphene contents. Table 1 also shows that there are no obvious change in melting temperatures and cold crystallization temperature of PVA in the nanocomposites. With the addition of graphene in the nanocomposites, the glass transition temperature (T_g) of PVA increases gradually from 76 °C to 90 °C, which could be attributed to the reduced mobility of polymer chains [25]. The increase in T_g indicates an effective attachment of PVA to the nanosheets of graphene that constrains the segmental motion of the polymer chains [20,26]. Moreover, ΔH_m and ΔH_c are strongly influenced by the graphene contents. The degree of crystallinity (X_c) is calculated from the ratio $\Delta H_m/\Delta H_0$, which are the measured and the 100% crystalline melting enthalpy, respectively. The melting enthalpy of a 100% crystalline PVA, ΔH_0, is taken as 138.6 J/g [27]. The crystallinity of PVA in the nanocomposites is determined by considering the weight fraction of PVA in the nanocomposites. The crystallinity of PVA in the nanocomposites decreases from 38.3% to an almost amorphous material at 3.5 wt% of graphene, supporting the hypothesis for the existence of some interaction between the polymer and graphene to the detriment of interactions among polymer chains. A high degree of crystallinity makes polymer brittle, it is because of the decrease in crystallinity that the films are more flexible, which will be discussed in the next part. In addition, ΔH_c decreases significantly as the graphene content increases in the nanocomposites, which indicates that the crystallization of PVA is retarded in the DSC cooling scans. The differences in crystallization behaviors observed for the nanocomposites can be explained considering the existence of interactions between graphene and the polymer matrix, which is consistent with FTIR and XRD experimental results previously discussed. In addition, the significant increase in T_g should result in lowered crystallization rates and may be reflected in the lower observed level of crystallinity.

TGA is further used to characterize the thermal properties of PVA and PVA/graphene nanocomposites (Fig. 4). The temperature of the maximum degradation rate for the nanocomposites (obtained from the derivative of TGA curves) is about 20–30 °C higher than that of pure PVA. These phenomena have been ascribed to the stability of the hydrogen bonding between polymer and graphene, which improves the thermal stability of PVA [28].

It is interesting to note that the structures and thermal properties of graphene/PVA nanocomposites were not the only aspect of the composites influenced. Since PVA is a semicrystalline polymer, its mechanical properties strongly depend on the degree of its crystallinity [29]. As discussed above, the crystallinity of PVA decreases with the increase of graphene in the nanocomposite. On the other hand, it is expected that the mechanical performance of the nanocomposite should be enhanced by the large aspect ratio of the graphene sheets, the molecular-level dispersion of the graphene sheets in PVA matrix, and strong interfacial interaction mainly by hydrogen bonding between graphene and PVA matrix. The typical stress–strain behaviors for the films of PVA, PVA/0.5 wt % graphene nanocomposite and PVA/3.5 wt% graphene nanocomposite are presented in Fig. 5 and Table 2. Compared with the pure PVA film, the tensile stress and modulus of PVA/3.5 wt% graphene nanocomposite mildly increase by 32% and 16%, respectively. The elongation at break of the nanocomposite films gradually

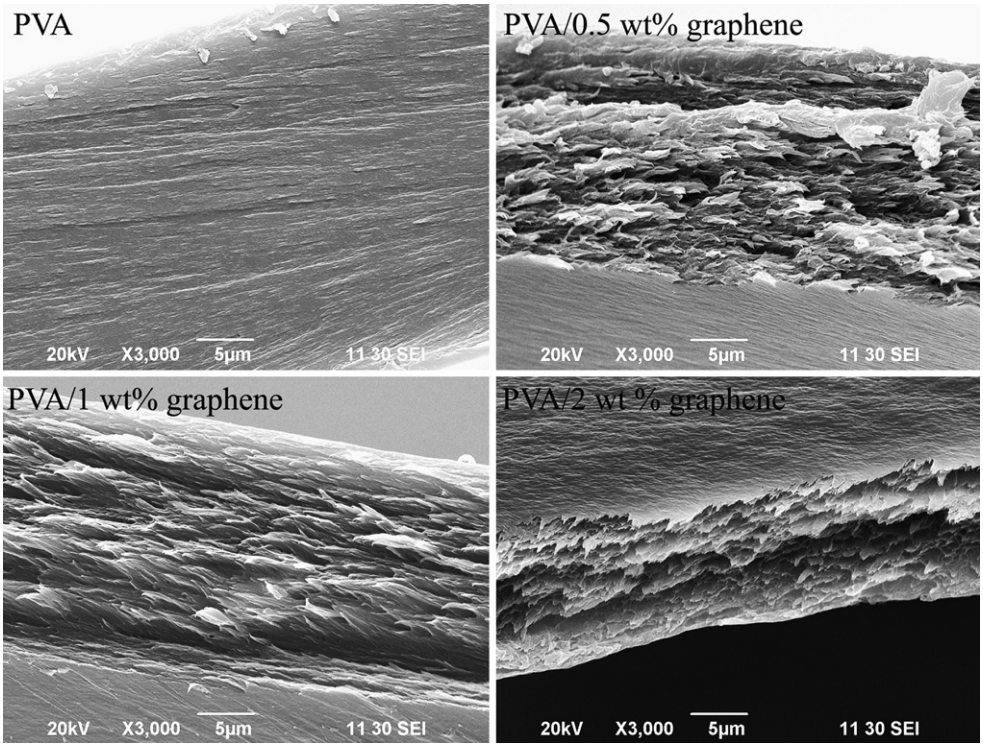

Fig. 6. SEM images of the fracture surface of PVA and PVA/graphene nanocomposite films.

decreases with increasing graphene content. The PVA/graphene nanocomposite films exhibit relatively large elongation at break though the values are smaller than that of PVA film. Therefore, the decrease in PVA crystallinity does not reduce the mechanical properties of the PVA/graphene nanocomposite films. The increase to some extent of the stress and modulus of the PVA/graphene nanocomposite films can be ascribed to the homogeneous dispersion of graphene sheets in the polymer matrix and strong interfacial interactions between both components. Similar results have been observed for polymer/carbon nanotubes nanocomposites [30]. Causin et al. reported that when carbon nanotubes were properly functionalized they could cooperate to the formation of an ordered structure and then a great increase in properties was obtained [31,32].

The fracture surfaces of the PVA/graphene nanocomposite films are further investigated by SEM after tensile testing. As shown in Fig. 6, the pure PVA is characterized with smooth surface and does not exhibit any preferential orientation. In contrast, the SEM images of the fracture surfaces of the PVA/graphene nanocomposite films clearly reveal layered-structures with uniformly dispersed graphene sheets in PVA matrix. These phenomena are different with those of the films of the polymer/carbon nanotubes composites [33]. They tend to align parallel to the film surface with the addition of graphene, just like that of the GO paper and membrane [34,35]. The preferential orientation of graphene may originate from gravitational forces experienced by the plate-like nanosheets. It has been reported that GO sheets could be piled up in a near-parallel manner, resulting in the formation of an ultrastrong paper-like material with a layered structure. Unfortunately, this material is brittle and it breaks at a small elongation [34,35]. In our case, it has been demonstrated that the nanocomposites of polymer and graphene with layer-aligned structure can combine the ductile property of polymer matrix and high strength of graphene sheets.

4. Conclusions

In conclusion, we have successfully prepared layer-aligned PVA/graphene nanocomposites by the reduction of graphene oxide in the presence of PVA and subsequently cast from aqueous solution. Though the addition of graphene significantly decreases the crystallinity of PVA, the film of the PVA/graphene nanocomposite is strong and ductile. The modulus and tensile stress of PVA/3.5 wt% graphene nanocomposite are 16% and 32% higher than those of pure PVA. And the glass transition temperature and the thermal stability are improved to some extent. On the basis of the results, the influence in the thermal and mechanical properties of the nanocomposites can be ascribed mainly to the homogeneous dispersion and alignment of graphene in PVA matrix and the interactions between both components. It demonstrates that graphene can be utilized effectively as thin two-dimensional nanosheets within the polymer matrix for the large-scale potential applications for polymer/graphene nanocomposites.

Acknowledgments

The work is supported by a grant (Economic Production of Carbon Nanotubes) of The Hong Kong Polytechnic University, Key Project in Science & Technology Innovation Cultivation Program of Soochow University, Educational Bureau of Hubei Province (Q20091508), Scientific Research Foundation for Returned Overseas Chinese Scholars of MOE ([2009]1341), Scientific Research Key Project of MOE (209081) and National Natural Science Foundation of China (20904044).

Appendix. Supplementary material

The supplementary data associated with this article can be found in the on-line version at doi:10.1016/j.polymer.2010.05.034.

References

[1] Novoselov KS, Jiang Z, Zhang Y, Morozov SV, Stormer HL, Zeitler U, et al. Science 2007;315(5817). 1379–1379.
[2] Lee C, Wei XD, Kysar JW, Hone J. Science 2008;321(5887):385–8.
[3] Heersche HB, Jarillo-Herrero P, Oostinga JB, Vandersypen LMK, Morpurgo AF. Nature 2007;446(7131):56–9.
[4] McAllister MJ, Li JL, Adamson DH, Schniepp HC, Abdala AA, Liu J, et al. Chem Mater 2007;19(18):4396–404.
[5] Li D, Kaner RB. Science 2008;320(5880):1170–1.
[6] Yu AP, Ramesh P, Itkis ME, Bekyarova E, Haddon RC. J Phys Chem C 2007;111 (21):7565–9.
[7] Vickery JL, Patil AJ, Mann S. Adv Mater 2009;21(21):2180–4.
[8] Verdejo R, Barroso-Bujans F, Rodriguez-Perez MA, Sajab JA, Lopez-Manchado MA. J Mater Chem 2008;18(19):2221–6.
[9] Stankovich S, Dikin DA, Dommett GHB, Kohlhaas KM, Zimney EJ, Stach EA, et al. Nature 2006;442(7100):282–6.
[10] Watcharotone S, Dikin DA, Stankovich S, Piner R, Jung I, Dommett GHB, et al. Nano Lett 2007;7(7):1888–92.
[11] Wang X, Zhi LJ, Mullen K. Nano Lett 2008;8(1):323–7.
[12] Liang JJ, Huang Y, Zhang L, Wang Y, Ma Y, Guo T, et al. Adv Funct Mater 2009;19(14):2297–302.
[13] Si Y, Samulski ET. Nano Lett 2008;8(6):1679–82.
[14] Salavagione HJ, Martinez G, Gomez MA. J Mater Chem 2009;19(28):5027–32.
[15] Han YQ, Lu Y. Composite Sci Technol 2009;69(7–8):1231–7.
[16] Shen JF, Hu YH, Li C, Qin C, Ye MX. Small 2009;5(1):82–5.
[17] Schniepp HC, Li JL, McAllister MJ, Sai H, Herrera-Alonso M, Adamson DH, et al. J Phys Chem B 2006;110(17):8535–9.
[18] Cao AN, Liu Z, Chu SS, Wu M, Ye Z, Cai Z, et al. Adv Mater 2010;22(1):103–6.
[19] Hummers WS, Offeman RE. J Am Chem Soc 1958;80:1339.
[20] Ramanathan T, Abdala AA, Stankovich S, Dikin DA, Herrera-Alonso M, Piner RD, et al. Nat Nanotechnol 2008;3(6):327–31.
[21] Hassan HMA, Abdelsayed V, Khder AERS, AbouZeid KM, Terner J, El-Shall MS, et al. J Mater Chem 2009;19(23):3832–7.
[22] Garcia-Cerda LA, Escareno-Castro MU, Salazar-Zertuche M. J Non-Cryst Solids 2007;353(8–10):808–10.
[23] Lu LY, Sun HL, Peng FB, Jiang ZY. J Membrane Sci 2006;281(1–2):245–52.
[24] Chen Y, Zhang X, Yu P, Ma Y. Chem Commun; 2009:4527–9.
[25] Mbhele ZH, Salemane MG, Sittert C, Nedeljkovic JM, Djokovic V, Luyt AS. Chem Mater 2003;15(26):5019–24.
[26] Yao ZL, Braidy N, Botton GA, Adronov A. J Am Chem Soc 2003;125 (51):16015–24.
[27] Su JX, Wang Q, Su R, Wang K, Zhang Q, Fu Q. J Appl Polym Sci 2008;107 (6):4070–5.
[28] Matsuo Y, Hatase K, Sugie Y. Chem Mater 1998;10(8):2266–9.
[29] Cadek M, Coleman JN, Barron V, Hedicke K, Blau WJ. Appl Phys Lett 2002;81 (27):5123–5.
[30] Zhang XF, Liu T, Sreekumar TV, Kumar S, Moore VC, Hauge RH, et al. Nano Lett 2003;3(9):1285–8.
[31] Wang SF, Shen L, Zhang WD, Tong YJ. Biomacromolecules 2005;6(6):3067–72.
[32] Causin V, Yang BX, Marega C, Goh SH, Marigo A. Eur Polym J 2009;45 (8):2155–63.
[33] Causin V, Yang BX, Marega C, Goh SH, Marigo A. J Nanosci Nanotechnol 2008;8 (4):1790–6.
[34] Chen C, Yang QH, Yang Y, Lv W, Wen Y, Hou PX, et al. Adv Mater 2009;21 (29):3007–11.
[35] Dikin DA, Stankovich S, Zimney EJ, Piner RD, Dommett GHB, Evmenenko G, et al. Nature 2007;448(7152):457–60.